Published in final edited form as:
Birth Defects Res B Dev Reprod Toxicol. 2010 June ; 89(3): 188–200. doi:10.1002/bdrb.20241.

A Systems-Based Approach to Investigate Dose- and Time-Dependent Methylmercury-Induced Gene Expression Response in C57BL/6 Mouse Embryos Undergoing Neurulation

Joshua F. Robinson[1,3,5], **Zachariah Guerrette**[1,3,5], **Xiaozhong Yu**[1,3,5], **Sungwoo Hong**[1,3,5], and **Elaine M. Faustman**[1,2,3,4,5,*]

[1]Department of Environmental and Occupational Health Sciences, University of Washington, Seattle, Washington

[2]Center for Ecogenetics and Environmental Health, Seattle, Washington

[3]Institute for Risk Analysis and Risk Communication, Seattle, Washington

[4]Center on Human Development and Disability, Seattle, Washington

[5]Center for Child Environmental Health Risks Research, Seattle, Washington

Abstract

BACKGROUND—Aberrations during neurulation due to genetic and/or environmental factors underlie a variety of adverse developmental outcomes, including neural tube defects (NTDs). Methylmercury (MeHg) is a developmental neurotoxicant and teratogen that perturbs a wide range of biological processes/pathways in animal models, including those involved in early gestation (e.g., cell cycle, cell differentiation). Yet, the relationship between these MeHg-linked effects and changes in gestational development remains unresolved. Specifically, current information lacks mechanistic comparisons across dose or time for MeHg exposure during neurulation. These detailed investigations are crucial for identifying sensitive indicators of toxicity and for risk assessment applications.

METHODS—Using a systems-based toxicogenomic approach, we examined dose- and time-dependent effects of MeHg on gene expression in C57BL/6 mouse embryos during cranial neural tube closure, assessing for significantly altered genes and associated Gene Ontology (GO) biological processes. Using the GO-based application GO-Quant, we quantitatively assessed dose- and time-dependent effects on gene expression within enriched GO biological processes impacted by MeHg.

RESULTS—We observed MeHg to significantly alter expression of 883 genes, including several genes (e.g., Vangl2, Celsr1, Ptk7, Twist, Tcf7) previously characterized to be crucial for neural tube development. Significantly altered genes were associated with development cell adhesion, cell cycle, and cell differentiation–related GO biological processes.

CONCLUSIONS—Our results suggest that MeHg-induced impacts within these biological processes during gestational development may underlie MeHg-induced teratogenic and neurodevelopmental toxicity outcomes.

*Correspondence to: Elaine M. Faustman, Department of Environmental and Occupational Health Sciences, 4225 Roosevelt Way NE Suite 100, University of Washington, Seattle, WA 98105. faustman@u.washington.edu.

Additional Supporting may be found in the online version of this article.

Keywords

metals; gene expression; methylmercury; development neurulation; neural tube defects; cell cycle; toxicogenomics

INTRODUCTION

The embryonic developmental period known as neurulation represents the process of neural tube formation and closure, the precursor sequence of events for central nervous system (CNS) formation. Occurring during gestational day (GD) 21–28 in humans and GD 7–10 in the mouse (Rodier, 1995), neurulation consists of four conserved stepwise events: initiation, elevation, adhesion, and fusion of the neural tube (Copp et al., 2003). Through the use of mouse mutants, approximately 190 genes have been identified to be necessary for successful neurulation (Harris and Juriloff, 2007). These studies as well as other molecular investigations suggest specific conserved developmental signaling pathways, such as Wnt and Shh, play critical roles during neurulation. They regulate processes such as cellular proliferation and differentiation underlying neural tube morphogenesis. Pathways controlling cell adhesion, cytoskeleton organization, and apoptosis play necessary roles in neural tube development (Copp, 2005). Many of these pathways make up necessary elements of the 17 conserved signaling pathways critical for development (National Research Council, 2000).

Environmental challenges may disrupt the timing and/or expression of these early signaling pathways critical for neural tube development. This results in neural tube defects (NTDs) and other developmental aberrations, including cleft palate and limb defects. Identification of environmental factors (e.g., folate status, hyperthermia, antieliptics) that may increase or reduce risk of NTD development has been essential in preventing NTDs in the human population (Finnell et al., 2000). Toxicogenomic studies suggest gestational exposure to metals such as cadmium (Robinson et al., 2009) and alcohol (Green et al., 2007; Hard et al., 2005; Robinson et al., 2009) disrupt the expression of developmental genes in association with increased defects of the neural tube, mortality, and other adverse developmental outcomes. Assessing the dose-response relationship between environmental exposures and the disruption of specific processes essential for successful neurulation may provide information beneficial for determining the mechanism(s) that underlie developmental toxicity during early embryonic development. This information may also be useful for risk assessment.

Methylmercury (MeHg) is a well-characterized teratogen and neurodevelopmental toxicant (Burbacher et al., 1990; Myers and Davidson, 1998; Myers et al., 1998). Due to the high lipophilicity of MeHg and a near complete absorption rate from the maternal gastrointestinal tract to the blood, fetal exposures to MeHg can take place following maternal exposures to the compound. Exposure occurs most commonly through the consumption of contaminated fin- and shellfish (Mozaffarian and Rimm, 2006). In humans, in utero exposures to high doses of MeHg can lead to cerebral palsy-like symptoms, mental retardation, and changes in primitive reflexes (Mergler et al., 2007). Studies using animal models propose MeHg to effect several biological pathways critical for development including cell proliferation, differentiation, oxidative stress signaling, and cytoskeleton organization (Castoldi et al., 2008; Faustman et al., 2002; Gribble, 2005; Gribble et al., 2005; Lewandowski et al., 2002; Ou et al., 1997, 1999; Ponce et al., 1994). Numerous studies have assessed the mechanistic link between MeHg and CNS developmental changes (Myers and Davidson, 1998; Myers et al., 1998); however, fewer studies have focused specifically on early gestational periods like neurulation. In animal models, MeHg exposures during early gestation can result in the

development of NTDs (Li et al., 1998; O'Hara et al., 2002; Papaconstantinou et al., 2003; Spyker and Smithberg, 1972; Su and Okita, 1976a), cleft palate (Li et al., 1998; O′Hara et al., 2002; Olson and Massaro, 1977, 1980; Su and Okita, 1976b), eye abnormalities (O′Hara et al., 2002), neurobehavioral modifications (Dore et al., 2001; Stoltenburg-Didinger and Markwort, 1990), and classic adverse birth outcomes, such as body weight changes and mortality. These developmental effects occur in a dose-dependent manner. For example, in 129/SvSl mice, prenatal maternal exposure to MeHg of 2 or 4 mg/kg BW (single ip injection, between GD 6–13) results in moderate increases in resorptions, fetal abnormalities (<1%), and body weight changes, while 8 mg/kg BW causes a significantly higher rate of resorptions, fetal abnormalities (8.7%), decreased fetal body weight (9%), as well as cleft palate (30.1%), neural tube defects (18.1%), and limb and facial malformations (Spyker and Smithberg, 1972). Additional studies provide evidence for single exposures of <5 mg/kg MeHg to produce minimal to mild toxicity, with doses of 8 or 10 mg/kg producing high rates of mortality, cleft palate, and other defects (O′Hara et al., 2002; Olson and Massaro, 1977).

Microarray analysis provides a unique approach to assess global gene expression changes across dose and time during early gestation. Initial microarray studies assessing untreated mouse brain across development (GD 12 to postnatal day 0), suggest robust time-dependent changes in genes related to CNS development, including genes related to synapse formation, axon growth, migration, polarity, differentiation, and survival (Matsuki et al., 2005). Changes in gene expression in this study matched prior knowledge of CNS development indicating the power and ability of microarray to assess gene expression changes across development. These types of studies show promise in proposing new targets of interest for biomarkers of exposure and early indicators of disease development. More recent studies have applied this technology to assess the role of environment factors in neural tube defects and developmental toxicity (Robinson et al., 2009; Wlodarczyk et al., 2006).

In the present study, we investigated dose- and time-dependent gene expression alterations associated with MeHg exposure, which induce minimal to high teratogenic developmental effects in C57 mouse embryos during early neurulation. Using a systems-based approach, we identified biological processes/pathways impacted by metal exposure that may underlie MeHg toxicity. We evaluated gene expression changes in enriched pathways previously identified to be active in the successful morphogenesis of the neural tube and early CNS development, including developmental signaling, cell proliferation and differentiation, and cell adhesion pathways. Our results not only indicate that MeHg impacts, in a dose- and time-dependent manner, pathways and genes previously identified to be critical for neural tube development but also propose new targets to be further investigated in MeHg-induced teratogenesis.

METHODS

Animals and Methylmercury Exposure

C57BL/6J (Jackson Labs, Bar Harbor, ME) rodent colonies were maintained at the University of Washington, Department of Environmental and Occupational Health Sciences, as previously described (Robinson et al., 2009). Mice were housed in filter-covered transparent plastic cages inside climate-controlled rooms under an alternating 12 h light/dark cycle, with water and food available ad libitium. Timed matings were encouraged by placing single male mice into cages holding two females in the late afternoon (~5 pm). Copulatory plugs were identified in the early morning (8:00 am ± 1 h) the following day and designated as GD 0. Pregnant mice were administered single doses by intraperitoneal injection on GD 8.0, 8:00 am (±1h), with either 0, 1, 4, or 6 mg/kg/BW Methylmercury Hydroxide (Alfa Aesar, Ward Hill, MA) dissolved in deionized water (working concentration of 2mM) or

vehicle control (water, 10 μl/g BW). The administration time and methodology of exposure were chosen to coincide with cranial neural tube closure and represent a period where metals induce exencephaly in this mouse strain (Hovland et al., 1999; Machado et al., 1999; Robinson et al., 2009). Doses were chosen to induce a wide range of effects: minimal (1 mg/kg), modest (4 mg/kg), and high (6 mg/kg) developmental toxicity. Potential effects include alterations in growth, neural tube closure, and other adverse developmental outcomes (Robinson et al., 2009; Spyker and Smithberg, 1972; Su and Okita, 1976b). Higher doses (>6 mg/kg BW) were not considered due to reported high resorption rates and possible maternal toxicity. To be consistent with other metal exposure studies conducted in our lab, we used the intraperitoneal injection administration method (Robinson et al., 2009). We did not observe any abnormal maternal toxicity consequences of using this administration method.

RNA Isolation

Following 0 (GD 8.0), 8 (GD 8.3), or 12 (GD 8.5) post-injection (h), dams were euthanized and embryos were isolated and washed in cold CMF-PBS, placed in liquid nitrogen, and stored at −80°C. Pooled litters of embryos were kept separate, placed in 500 μl of RTL Cell Lysis buffer (Qiagen, Valencia, CA), and lysed with a 30G needle to homogenize the tissue. RNA was purified using the RNAeasy kit (Qiagen, Valencia, CA) according to the manufacturer's protocol. RNA quality and quantity were assessed using Nanodrop ND-100 spectrophotometer (Nanodrop Technologies, Wilmington, DE) and the "6000" assay on the 2100 Bioanalyzer (Agilent Technologies, Palo Alto, CA). For each dose and time-point, RNA was collected from three to five separate litters (n = 3–5, per group) (see Suppl. Table S1, available online at www.interscience.wiley.com). The 1 mg/kg group was assessed only at 8 h due to array availability.

Oligonucleotide Microarrays

Using 1 μg of total RNA from each litter, we performed microarray analysis using Mouse 430 2.0 Arrays (Affymetrix, Inc., Santa Clara, CA). Microarray hybridizations were completed using the GeneChip One-Cycle Target Labeling kit (Affymetrix, Inc.) following the manufacturer's protocol. The amount and quality of the cRNA were assessed using a Nanodrop ND-100 spectrophotometer and an Agilent Bioanalyzer (Agilent Technologies, Palo Alto, CA). Prior to washing and scanning, cRNA was fragmented and hybridized to the arrays for 17 h.

Data Processing

Intensity values were extracted from scanned images using GeneChip Operating Software (Affymetrix, Inc.) for all 45,101 probes included on the arrays. Raw intensities were normalized using GC-Robust Multiarray Averaging (GC-RMA) and transformed by log base 2 (BRBarraytools, NCI).

Identification of Significantly Altered Genes Using ANOVA

To explore MeHg-dependent alterations, we employed a discrete linear model to assess genes that were impacted by MeHg across dose and time:

Model: $\text{Log}_2[\text{Exp}_n]_{\text{C57BL/6J}} = \beta_{\text{MeHg}}x_1 + \beta_{\text{Time}}x_2$

Dose effect (β_{MeHg}), x_1 = {con = 0, 1 mg/kg = 1, 4 mg/kg = 2, 6 mg/kg = 3}

Time effect (β_{Time}), x_2 = {0h = 0, 8h = 1, 12h = 2}

Using the model above, we employed a P value cutoff (ANOVA, F-test, P<0.0005) for the primary treatment term (β_{MeHg}) to identify genes that were significantly altered due to

MeHg exposure across dose and time (Supp. Fig. S1). For each probe identified to be significantly altered by MeHg, $\log_2$ ratios were calculated in comparison between each array and its respective concurrent control (either 8 or 12 h). We chose the above criteria to analyze ~2% of all probes, or 883 individual probes, represented on the Affymetrix platform. Approximately 10% of the 883 individual probes identified to be significantly altered by MeHg were represented as duplicates or triplicates of unique genes, amounting to ~800 unique genes being affected. Since the number of genes represented by multiple probes makes up a relatively small proportion of the genes impacted by MeHg, we referred to them as genes, rather than probes, in this report to simplify the language used herein. To visualize changes in gene expression across dose and time, hierarchical clustering analysis was conducted for all 883 genes using average linkage and Euclidean dissimilarity methods (TIGR MEV, http://www.tm4.org/mev.html) (Eisen et al., 1998). Two-sided student's t-tests were completed between each treatment group and respective concurrent control to determine dose- and time-related responses within the 883 genes identified to be significantly altered with MeHg across dose and time.

Functional Interpretation of Significantly Altered Genes Using GO and Pathway Analysis

Gene Ontology (GO) analysis (MAPPFinder, Gladstone Institutes, UCSF; http://www.genmapp.org) (Doniger et al., 2003) was conducted to identify enriched GO categories, classified by biological process, molecular function, and cellular component, within significantly differentially expressed genes identified to be altered with MeHg exposure (β_{MeHg}, $P<0.0005$). Approximately 50% of all "significantly" altered genes were linked to a GO term within the GO hierarchy. Significantly altered categories were identified based on the permutation P value ≤0.001, Z-score >2, and a minimum of 5 genes changed within each specific GO ID. We used the GO-based application, GO-Quant (Institute for Risk Assessment and Risk Communication, University of Washington; http://depts.washington.edu/irarc/Go-Quant/index.html) (Yu et al., 2006) to quantitatively evaluate functional changes within gene-expression linked GO categories. GO-Quant was also used to calculate the absolute average fold change (FC) between each MeHg exposure group and to control for all significantly altered genes within each enriched GO subset. Color-coded diagrams were created to display average $\log_2$ ratios between treatment groups to compare the average treatment group and its respective control (8 or 12 h). Ordered by the GO hierarchical system (AmiGO, Gene Ontology Consortium; http://amigo.geneontolo-gy.org/) (Carbon et al., 2009) significant categories with $150 > X > 6$ significantly MeHg-impacted genes were identified. For selected enriched GO categories, specifically developmental process, cell adhesion, cell differentiation, and cell cycle, we conducted hierarchical clustering of $\log_2$ ratios of all significantly altered genes within selected enriched GO terms across dose groups at 8 and 12 h. Pathway analysis was conducted to explore MeHg-impacted genes within the Wnt-signaling pathway (DAVID, http://david.abcc.ncifcrf.gov/) (Dennis et al., 2003). Overrepresented transcription factor–binding sites (TFBS) within genes identified to be significantly altered by MeHg were identified using oPPOSSUM (mouse, vertebrate, default criteria) (Ho Sui et al., 2005). Approximately 70% of MeHg-altered genes were linked with the TFBS database. All TFBS with a Z-score >10 represented by more than 10 genes were selected as enriched.

RESULTS

MeHg-Induced Dose- and Time-Dependent Alterations in Gene Expression

In Figure 1, we show the distribution of significant MeHg-induced gene expression alterations across dose and time based on a P value cutoff of 0.0005 (ANOVA, F-test, β_{MeHg}). We identified 883 genes to be significantly altered with MeHg across dose and time (black bar). Within these 883 genes, post-hoc analyses (t-test) were conducted to identify the

number of genes within each treatment group to be significantly altered in comparison with the appropriate concurrent control (8 or 12 h control). We identified a dose-dependent increase in the percentage of genes identified to be altered within each dose group (*t*-test, $P<0.05$) at both 8 and 12 h, in relation to the total amount of genes (883 genes) identified to be significantly altered across all dose groups. With 6 mg/kg, we observed a similar response in the amount of genes significantly altered at 8 and 12 h.

In Figure 2, we show hierarchical clustering plots of all genes identified to be impacted by MeHg across dose at 8 and 12h. Diagrams present $\log_2$ ratios of intensities comparing each array and their respective concurrent control (8- or 12 h control). At 8 and 12 h, we observed dose-dependent alterations in gene expression levels compared to controls, with consistent changes occurring in the highest dose (6 mg/kg) group for the majority of genes at both timepoints. Variability within experimental groups was observed within lower dose groups, including array "A" MeHg 1 mg/kg and array "D" MeHg 4 mg/kg. Hierarchical clustering by sample indicated these arrays were more similar to 8- and 12h controls (not shown). In general, we observed that genes were either consistently upregulated or downregulated with MeHg exposure across dose at the two timepoints investigated.

Quantitative GO Analysis of MeHg-Induced Gene Expression Alterations

Using the Gene Ontology (GO) hierarchical classification system, we identified enriched biological processes/pathways (GOIDs) within the collection of genes identified as significantly altered with MeHg exposure across dose and time. In summary, MeHg induced alterations in genes representing several biological processes/pathways, including: development processes relating to CNS, neural tube, muscle, anterior/posterior pattern formation, and the Wnt signaling pathway; protein and RNA metabolic processes; and cell cycle, cell adhesion, cell differentiation, cell communication, and cellular organization (cellular localization, actin cytoskeleton).

As presented in Figure 3, using GO-Quant, we quantitatively assessed the absolute magnitude in change of expression levels associated with significant genes within enriched GO biological processes/pathways across dose at 8 and 12 h. We observed a dose-dependent increase in the absolute average fold change in gene expression across dose (log 2 scale) at both timepoints. At 8 h, the average magnitude in change (absolute $\log_2$ ratios) associated with each enriched GO category varied between 1 and 4 mg/kg treatment groups, but consistently showed the largest changes in the 6 mg/kg group (relative to control). At 12 h, a greater magnitude of effect was also observed in the 6 mg/kg MeHg group compared to the 4 mg/kg group. For the 6 mg/kg MeHg group, responses relative to the appropriate controls at 12 h were less than values at 8 h. In contrast, all fold change values associated with 4 mg/kg were higher at 8 h compared to 12 h. The most extreme changes in degree of magnitude at both 8h (> 0.70 $\log_2$ ratio) and 12 h (> 0.62 $\log_2$ ratio) were observed within genes related to cell adhesion (GO categories: homophilic cell adhesion, cell–cell adhesion, cell adhesion, biological adhesion), cellular component organization and biogenesis (GO categories: regulation of cellular component organization and biogenesis, negative regulation of cell organization and biogenesis, protein depolymerization, microtubule cytoskeleton organization and biogenesis), and developmental processes (GO categories: anterior/posterior pattern formation, neural tube development).

In Figure 4, we present hierarchical clusters of expression values for individual gene expression within enriched GO biological processes, Developmental Process (A) and Cell Adhesion (B), to determine the dose-response and directional change in magnitude of gene expression within each respective GO category as a result of MeHg dose at 8 and 12 h. We identified ~15% (134genes) of all MeHg-altered genes (~28% of genes linked with a GOID) to be linked with the GO-biological process, "developmental process" (Fig. 4A). Within this

subset, we observed alterations of genes known to be involved in neural tube development (+), Wnt signaling ($), and anterior/posterior pattern formation (#) across all MeHg doses. For example, we identified 21% of linked neural tube development genes (9/43 genes measured) to be altered by MeHg, including Ptk7, Celsr1, Grif1, Twist1, Tcf7l2, Tcf7, Gli2, Vangl2, and Nf1, with all up-regulated in expression. In Figure 4B, we show that 32 genes related to cell adhesion were impacted by MeHg dose at the time-points investigated. Genes specifically involved in homophilic cell adhesion genes (−) included both genes that were upregulated (Fbn2, Celsr1, Dchs1, Fat1, Pcdh19, Frem2, Fat4, Clstn1, Pcdh7) and downregulated (6820431F20Rik) as a result of MeHg treatment. We identified alterations in genes previously identified to be associated with NTD formation in knockout mouse models (Harris and Juriloff, 2007) in both developmental process and cell adhesion–related GO biological processes,. These included 18 genes identified in knockout models to be crucial for neural tube closure: Celsr1, Ptk7, Smarcc1, Smarca4, Grlf1, Twist1, Hipk1, Ep300, Frem2, Dync2h1, Hdac4, Vangl2, Nf1, Ski, Sufu, Tcf7, Tcf7l2, Gli2. For the majority of responses in these two categories, we observed greater magnitudes in expression changes with the 6 mg/kg dose compared to the 1- and/or 4 mg/kg doses. The majority of genes in these two categories were upregulated at both 8 and 12 h with MeHg.

In Figure 5, we demonstrate the dose-dependent impact of MeHg on genes related to the Wnt-signaling pathway (8h) to observe potential interactions on a pathway-based level (Figure 5). As observed with our GO analyses, the majority of Wnt-signaling pathway members were observed to be upregulated with MeHg.

We identified gene expression alterations within enriched GO categories, Cell Differentiation (A) and Cell Cycle (B) clusters, to determine the dose-response and directional change in magnitude in genes within these GO categories with treatment with MeHg (Fig. 6). We identified ~10% (90 genes) of all genes significantly altered by MeHg to be associated with the GOID, cell differentiation (Fig. 6A). Ninety percent of cell differentiation genes were identified to be linked with the GO term, developmental process. Additionally, we observed 42 genes related to cell cycle to be impacted by MeHg (Fig. 6B). For the majority of responses in these two categories, we observed greater magnitudes of expression changes within the 6 mg/kg dose group of arrays (8 or 12 h). The majority of genes in these two categories were upregulated at both 8 and 12 h with MeHg. Descriptions of selected genes identified within Figures 4 and 6 are presented in the Discussion section.

DISCUSSION

MeHg is a well-characterized teratogen and neurodevelopmental toxicant able to induce a wide range of developmental alterations, including neurobehavioral changes, growth effects (birth weight, size), and malformations such as NTDs (exencephaly), cleft palate, and eye abnormalities. In this study, we investigated the dose-dependent impact of MeHg on gene expression within C57 mouse embryos exposed during the neurulation period of development. Using a systems-based approach, we identified dose- and time-dependent effects on the expression of genes associated with biological processes/pathways, including neural tube development, Wnt signaling, polarity, cell adhesion, cell cycle, and cell differentiation, previously identified to be crucial for successful neurulation. Here, we discuss our results in relation to the neurulation process and suggest MeHg impacts, which may underlie toxicity and developmental outcomes.

Neurulation is thought to consist of four conserved stepwise events: initiation, elevation, adhesion, and fusion of the neural tube (Copp et al., 2003). Initiation of neural tube closure involves the shaping of the neural plate determined by convergent extension cellular movements, which result in narrowing and lengthening of the neural plate. Controlling these

initial cellular movements, genes such as Celsr1-3, Fzd3, Fzd6, Scrb1, Ptk7, Vangl1-2, Dvl1-3, and Wnt5a are implicated as interacting members within the mammalian planar cell-polarity (PCP) pathway also known as the non-canonical Wnt/frizzled signaling pathway (Copp et al., 2003; Montcouquiol, 2007; Montcouquiol et al., 2006, 2008; Qian et al., 2007; Tissir and Goffinet, 2006; Zhou et al., 2007). We identified significant upregulation of PCP pathway members Celsr1, Vangl2, Ptk7, and Wnt5a with MeHg exposure in a dose- and time-dependent manner (Fig. 4A, B), indicating possible disruption of this pathway. Knockout models of Celsr1, Vangl2, Ptk7, and Wnt5a display increased craniorachischisis, a congenital fissure of the spinal column and skull, and cochlear alterations (Curtin et al., 2003; Lu et al., 2004; Murdoch et al., 2001; Qian et al., 2007; Torban et al., 2008), indicating the importance and the needed stability of this gene network for early development. Many of these genes continue to be essential for later stages of CNS development. For example, the 7-pass transmembrane G protein–coupled receptor, Celsr1, plays a role in axonal development, specifically expressed in the ventricular zone and external granular layers, areas of high neuronal precursor cell proliferation and differentiation (Tissir et al., 2002). Environmental disruption of PCP members also suggests a link with perturbations in development. For example, following exposure to retinoic acid on GD9.5, mouse (Balb/C) fetuses display lower Vangl2 expression in the cranial posterior neuropore in association with 100% development of the NTD exencephaly (Liu et al., 2008). Disruption of this pathway, as suggested by the current study, may underlie the etiology of NTDs, fetal mortality, and other developmental abnormalities induced as a result of environmental exposures to MeHg.

Elevation and subsequent bending of the neural folds is dependent on the hedgehog (Shh) signaling pathway. Secreted from notochord and floor plate, Shh induces Gli-transcription factors, which, through the patched receptor, increase expression of Wnt-pathway modulators and deactivate signaling molecules that repress Shh signaling (Ruiz i Altaba et al., 2003). Across the doses and time points investigated in the current study, MeHg significantly induced Gli2 and Sufu expression (Fig. 4), both of which are interacting members of the Shh pathway. Gli2 belongs to the zinc-finger class of transcription factors and is highly expressed in the developing neural tube as well as the surrounding mesodermal tissues. Knockout models suggest expression of Gli2 is crucial for proper brain, craniofacial, lung, and skeletal development (Ding et al., 1998; Matise et al., 1998; Mo et al., 1997). Sufu represses Gli transcription factors by sequestering Gli proteins in the cytoplasm or by directly inhibiting Gli-mediated transactivation (Stone et al., 1999). Shh counteracts the activity of Sufu by inducing turnover of the active protein via the ubiquitin proteasome system (Yue et al., 2009) thus allowing Gli2-mediated transcription to take place. The regulation of the Shh pathway is critical for survival, as Sufu (−/−) mice display NTDs and do not live past GD 10 (Cooper et al., 2005). Disruption of the interactions between Shh pathway members as a result of MeHg exposure may underlie induced alterations occurring during neurulation.

Interactions between the canonical Wnt and Shh signaling pathways are critical for normal morphogenesis and development because they regulate dorsal-ventral patterning along the neural tube in the early developing embryo (Alvarez-Medina et al., 2008). As shown in Figure 4A, we observed several members of the GO biological process, Wnt signaling pathway (identified with the $ symbol) to be altered by MeHg exposure, including up-regulation of Tcf7l2, Tcf7, Fzd1, Fzd7, Sfrp1, Sfrp2, Lef1, Macf1, Apc, Wnt5a, Lrp1, and 0610010D24Rik. Further examination of expression changes in the Wnt-signaling pathway shows consistent up-regulation of interacting members (Fig. 5), suggesting a significant and consistent modulation by MeHg. Wnt ligands bind to frizzled (Fzd) receptors beginning a signaling cascade that involves Apc and Macf1 among others. These, in turn, activate the translocation of β-catenin into the nucleus to form complexes with Tcfs/Lef and other

factors, activating transcription of Wnt target genes that control proliferation and differentiation (i.e., Pten, Myc) (Behrens et al., 1996). Genes such as 060010D24Rik (Oshita et al., 2003), which induces β-catenin cytoplasmic stabilization and extracellular wnt ligand inhibitors Sfrp1 and Sfrp2 (Wawrzak et al., 2007), modulate Wnt downstream signaling. Preliminary investigations assessing enrichment of TFBS within genes identified to be significantly altered by MeHg ($P > 0.0005$), suggest potential disruption of several transcription factors (e.g., Foxd3, Foxa2, Sox17) known to interact with both Shh and Wnt signaling pathways (Suppl. Table S2). These observations may be useful in planning additional studies to further determine the role of MeHg in altering Shh and Wnt signaling pathways, both critical pathways for neurulation and embryogenesis.

Fusion of the neural folds depends on the initial adhesion and the establishment of cellular contacts. Following elevation of the neural folds, specific molecules are expressed (e.g., cadherins) that promote the joining of cells in the neural folds of the neuroepithelium and mesenchymal regions. Cell adhesion genes have been identified to be critical for proper adhesion and fusion of the neural tube as well as craniofacial development (cleft palate) (Harris and Juriloff, 2007; Juriloff and Harris, 2008). Here, we identified MeHg as capable of significantly disrupting cellular adhesion pathways in a dose- and time-dependent manner (Fig. 4B), including genes linked with both NTD development and cleft palate, such as Vangl2, Ptk7, Twist1, Celsr1, and Frem2 (Harris and Juriloff, 2007). Previous studies in embryonic human stem cells suggest MeHg to induce a reduction in expression of the cadherin molecule Ncam1 (Stummann et al., 2009). This protein regulates tissue development during neurulation and later CNS development (Buttner and Horstkorte, 2008). Supporting these in vitro observations, we identified the following alterations in gene expression: several cadherins, such as Fat1, Fat4, Dchs1, Ctnnd1, and 6820431F20Rik; protocadherins like Pcdh19 and Pcdh7; collagens including Col13a1 and Col18a1; glycoproteins, such as Fb1, Hspg2, and Vcan; and other factors that regulate cellular organization, including Dab1, Dst, Grlf1, Hspg2, Itga4, Neo1, Frem2, Twist1, Vangl2, Celsr1, and Ptk7. The large collection of cell-adhesion genes impacted by MeHg suggests that disruption of these processes during this time in development potentially leads to incomplete closure of the neural tube, with associated morphological abnormalities.

Regulatory pathways controlling cellular proliferation and differentiation during development are vital for proper morphogenesis, including neurulation. Several knockout models of genes that regulate the balance between proliferation and differentiation during early development display neural tube defects and other developmental aberrations (Harris and Juriloff, 2007). For example, expansion of the cranial mesenchyme is dependent on high rates of cellular proliferation and expansion during this period. Knockouts of Twist1, a transcription factor that negatively regulates cell determination, result in a reduction in the proliferation of cells and expansion of cell layers within the mesenchymal region, leading to exencephaly (Chen and Behringer, 1995). Genes regulating these processes have been shown to be altered as a result of metal-induced toxicity and MeHg's effects on cellular proliferation and differentiation have been well documented in whole animal and in vitro models (Faustman et al., 2002). For example, MeHg was shown to inhibit neuronal differentiation in neural stem cells isolated from GD 15 rat embryos (Tamm et al., 2006). Stummann et al. (2009) showed that MeHg could disrupt levels of neuronal differentiation markers, suppressing expression of Ncam1, Neurod1, and Map2 in particular, at exposures that did not generate cytotoxicity. Additionally, in MeHg-exposed C57 embryos (GD 8.0, intraperitoneal injection, 4 mg/kg BW), we have shown MeHg to induce expression of p53 and Cdkn1a (Robinson et al., unpublished data). In fact, the magnitude of MeHg-induced toxicity in primary cultures of mouse neuronal precursor cells and embryonic fibroblasts has been shown to be dependent on the presence of genes that regulate cell-cycle exit (p53, Cdkn1a) (Gribble, 2005; Ou et al., 1999). In the present study, we did not observe

significant induction of p53 or Cdkn1a with prenatal exposure to MeHg. However, we observed upregulation of Ep300, Prkdc, and Atr, all known activators of p53 expression (Bode and Dong, 2004) (Fig. 4B). How alterations in the expression of these genes may result in adverse developmental outcomes is still unclear. However, it has been proposed that MeHg may reduce cellular growth, altering cellular proliferation by (1) lengthening the cell cycle; (2) decreasing the dividing fraction time; (3) increasing cellular death; (4) decreasing intracellular biosynthesis; or (5) decreasing extracellular biosynthesis (Chen et al., 1979). In the present study, we report MeHg impacts within multiple genes regulating the dynamic balance of the proliferation and differentiation processes. These genes include MeHg-induced alterations in cell cycle genes (Ccne1, Cdc27, Wee1, Tgfb2, Anapc1, Cdk6, Hdac1, Smad3, Creb1, Smad2, and Prkdc), interacting members of the KEGG cell-cycle signaling pathway (not shown). Similar to previous studies, we show MeHg to disrupt expression of genes controlling cellular proliferation and differentiation.

The doses in this study were selected based on previous studies and intended to range from doses that did not induce significant developmental effects to doses that did induce outright toxicity (i.e., mortality and malformations). Our findings suggest a dose-response relationship in regards to the magnitude of impact and the number of genes altered with dose (Fig. 1). Additional experiments using doses in the lower end of the dose-response curve may improve our mechanistic evaluations of MeHg's mode of action in the developing organisms and may thus be ideal for benchmark calculations when considering developmental endpoints in risk assessments. Assessing lower doses using toxicogenomic analyses may also improve assessment of low-dose effects that may not induce significant toxicity in animal studies due to sample size limitations or experimental variability.

In this study, we have identified several processes that MeHg may disrupt in a dose- and time-dependent manner including developmental signaling pathways that have been previously identified to be involved in neurulation. This dataset reinforces the notion that MeHg-mediated developmental toxicity results from the disruption of a complex and varied set of processes and highlights the need of future studies to examine the cross-talk and intersections of these pathways in order to further elucidate the effects of MeHg and similar metallic compounds on the developing organism.

Supplementary Material

Refer to Web version on PubMed Central for supplementary material.

Acknowledgments

The authors thank Dr Edward K. Lobenhofer and Cogenics for conducting microarray hybridization for all Affymetrix arrays used in this study and Alison Laing for her editorial support. This work was supported in part by the National Institute of Environmental Health Sciences (NIEHS) (Toxicogenomics U10 ES 11387 and R01-ES10613 and Environmental Pathology and Toxicology Training Grant 5 T32 ES007032), the US Environmental Protection Agency-NIEHS UW Center for Child Environmental Health Risks Research (EPA R826886 and NIEHS 1PO1ES09601), the Center for Oceans and Human Health Research (NIEHS: P50 ES012762), the National Science Foundation (NSF: OCE-0434087), NIEHS and the UW Center for Ecogenetics and Environmental Health (5 P30 ES07033).

REFERENCES

Alvarez-Medina R, Cayuso J, Okubo T, Takada S, Marti E. Wnt canonical pathway restricts graded Shh/Gli patterning activity through the regulation of Gli3 expression. Development (Cambridge, UK). 2008; 135:237–247.

Behrens J, von Kries JP, Kuhl M, Bruhn L, Wedlich D, Grosschedl R, Birchmeier W. Functional interaction of beta-catenin with the transcription factor LEF-1. Nature. 1996; 382:638–642. [PubMed: 8757136]

Bode AM, Dong Z. Post-translational modification of p53 in tumorigenesis. Nat Rev Cancer. 2004; 4:793–805. [PubMed: 15510160]

Burbacher TM, Rodier PM, Weiss B. Methylmercury developmental neurotoxicity: a comparison of effects in humans and animals. Neurotoxicol Teratol. 1990; 12:191–202. [PubMed: 2196419]

Buttner B, Horstkorte R. Intracelluar ligands of NCAM. Neurochem Res. 2008 Feb 21. [Epub ahead of print].

Carbon S, Ireland A, Mungall CJ, Shu S, Marshall B, Lewis S. AmiGO: online access to ontology and annotation data. Bioinformatics. 2009; 25:288–289. [PubMed: 19033274]

Castoldi AF, Onishchenko N, Johansson C, Coccini T, Roda E, Vahter M, Ceccatelli S, Manzo L. Neurodevelopmental toxicity of methylmercury: laboratory animal data and their contribution to human risk assessment. Regul Toxicol Pharmacol. 2008; 51:215–229. [PubMed: 18482784]

Chen WJ, Body RL, Mottet NK. Some effects of continuous low-dose congenital exposure to methylmercury on organ growth in the rat fetus. Teratology. 1979; 20:31–36. [PubMed: 515962]

Chen ZF, Behringer RR. twist is required in head mesenchyme for cranial neural tube morphogenesis. Genes Dev. 1995; 9:686–699. [PubMed: 7729687]

Cooper AF, Yu KP, Brueckner M, Brailey LL, Johnson L, McGrath JM, Bale AE. Cardiac and CNS defects in a mouse with targeted disruption of suppressor of fused. Development (Cambridge, UK). 2005; 132:4407–4417.

Copp AJ. Neurulation in the cranial region--normal and abnormal. J Anat. 2005; 207:623–635. [PubMed: 16313396]

Copp AJ, Greene ND, Murdoch JN. The genetic basis of mammalian neurulation. Nat Rev Genet. 2003; 4:784–793. [PubMed: 13679871]

Curtin JA, Quint E, Tsipouri V, Arkell RM, Cattanach B, Copp AJ, Henderson DJ, Spurr N, Stanier P, Fisher EM, Nolan PM, Steel KP, Brown SD, Gray IC, Murdoch JN. Mutation of Celsr1 disrupts planar polarity of inner ear hair cells and causes severe neural tube defects in the mouse. Curr Biol. 2003; 13:1129–1133. [PubMed: 12842012]

Dennis G Jr. Sherman BT, Hosack DA, Yang J, Gao W, Lane HC, Lempicki RA. DAVID: database for annotation, visualization, and integrated discovery. Genome Biol. 2003; 4:P3. [PubMed: 12734009]

Ding Q, Motoyama J, Gasca S, Mo R, Sasaki H, Rossant J, Hui CC. Diminished Sonic hedgehog signaling and lack of floor plate differentiation in Gli2 mutant mice. Development (Cambridge, UK). 1998; 125:2533–2543.

Doniger SW, Salomonis N, Dahlquist KD, Vranizan K, Lawlor SC, Conklin BR. MAPPFinder: using Gene Ontology and Gen-MAPP to create a global gene-expression profile from microarray data. Genome Biol. 2003; 4:R7. [PubMed: 12540299]

Dore FY, Goulet S, Gallagher A, Harvey PO, Cantin JF, D'Aigle T, Mirault ME. Neurobehavioral changes in mice treated with methylmercury at two different stages of fetal development. Neurotoxicol Teratol. 2001; 23:463–472. [PubMed: 11711249]

Eisen MB, Spellman PT, Brown PO, Botstein D. Cluster analysis and display of genome-wide expression patterns. Proc Natl Acad Sci USA. 1998; 95:14863–14868. [PubMed: 9843981]

Faustman EM, Ponce RA, Ou YC, Mendoza MA, Lewandowski T, Kavanagh T. Investigations of methylmercury-induced alterations in neurogenesis. Environ Health Perspect. 2002; 110(Suppl 5): 859–864. [PubMed: 12426147]

Finnell RH, Gelineau-van Waes J, Bennett GD, Barber RC, Wlodarczyk B, Shaw GM, Lammer EJ, Piedrahita JA, Eberwine JH. Genetic basis of susceptibility to environmentally induced neural tube defects. Ann NY Acad Sci. 2000; 919:261–277. [PubMed: 11083116]

Green ML, Singh AV, Zhang Y, Nemeth KA, Sulik KK, Knudsen TB. Reprogramming of genetic networks during initiation of the Fetal Alcohol Syndrome. Dev Dyn. 2007; 236:613–631. [PubMed: 17200951]

Gribble, EJ. Cell cycle inhibition as a mode of abnormal development: the role of cell cycle checkpoint proteins and cyclin-dependent kinase inhibitors in neurodevelopmental toxicant defense. Seattle: University of Washington; 2005.

Gribble EJ, Hong SW, Faustman EM. The magnitude of methylmercury-induced cytotoxicity and cell cycle arrest is p53-dependent. Birth Defects Res A Clin Mol Teratol. 2005; 73:29–38. [PubMed: 15641097]

Hard ML, Abdolell M, Robinson BH, Koren G. Gene-expression analysis after alcohol exposure in the developing mouse. J Lab Clin Med. 2005; 145:47–54. [PubMed: 15668661]

Harris MJ, Juriloff DM. Mouse mutants with neural tube closure defects and their role in understanding human neural tube defects. Birth Defects Res A Clin Mol Teratol. 2007; 79:187–210. [PubMed: 17177317]

Ho Sui SJ, Mortimer JR, Arenillas DJ, Brumm J, Walsh CJ, Kennedy BP, Wasserman WW. oPOSSUM: identification of over-represented transcription factor binding sites in co-expressed genes. Nucleic Acids Res. 2005; 33:3154–3164. [PubMed: 15933209]

Hovland DN Jr. Machado AF, Scott WJ Jr. Collins MD. Differential sensitivity of the SWV and C57BL/6 mouse strains to the teratogenic action of single administrations of cadmium given throughout the period of anterior neuropore closure. Teratology. 1999; 60:13–21. [PubMed: 10413334]

Juriloff DM, Harris MJ. Mouse genetic models of cleft lip with or without cleft palate. Birth Defects Res A Clin Mol Teratol. 2008; 82:63–77. [PubMed: 18181213]

Lewandowski TA, Pierce CH, Pingree SD, Hong S, Faustman EM. Methylmercury distribution in the pregnant rat and embryo during early midbrain organogenesis. Teratology. 2002; 66:235–241. [PubMed: 12397631]

Li Y, Pan Y, Zhu H. Relation between methylmercury chloride-induced programmed cell death and the development of nervous system in rats. Wei Sheng Yan Jiu. 1998; 27:241–244. (trans. from Chinese). [PubMed: 10682593]

Liu J, Qi J, Zhu J, Zhang L, Liang Y, Ning Q, Luo X. Effects of Retinoic Acid on the Expressions of Vangl1 and Vangl2 in Mouse Fetuses. J Neurogenet. 2008:1–12.

Lu X, Borchers AG, Jolicoeur C, Rayburn H, Baker JC, Tessier-Lavigne M. PTK7/CCK-4 is a novel regulator of planar cell polarity in vertebrates. Nature. 2004; 430:93–98. [PubMed: 15229603]

Machado AF, Hovland DN Jr. Pilafas S, Collins MD. Teratogenic response to arsenite during neurulation: relative sensitivities of C57BL/6J and SWV/Fnn mice and impact of the splotch allele. Toxicol Sci. 1999; 51:98–107. [PubMed: 10496681]

Matise MP, Epstein DJ, Park HL, Platt KA, Joyner AL. Gli2 is required for induction of floor plate and adjacent cells, but not most ventral neurons in the mouse central nervous system. Development (Cambridge, UK). 1998; 125:2759–2770.

Matsuki T, Hori G, Furuichi T. Gene expression profiling during the embryonic development of mouse brain using an oligonucleotide-based microarray system. Brain Res. 2005; 136:231–254.

Mergler D, Anderson HA, Chan LH, Mahaffey KR, Murray M, Sakamoto M, Stern AH. Methylmercury exposure and health effects in humans: a worldwide concern. Ambio. 2007; 36:3–11. [PubMed: 17408186]

Mo R, Freer AM, Zinyk DL, Crackower MA, Michaud J, Heng HH, Chik KW, Shi XM, Tsui LC, Cheng SH, Joyner AL, Hui C. Specific and redundant functions of Gli2 and Gli3 zinc finger genes in skeletal patterning and development. Development (Cambridge, UK). 1997; 124:113–123.

Montcouquiol M. Planar polarity in mammals: similarity and divergence with *Drosophila melanosgaster*. J Soc Biol. 2007; 201:61–67. (trans. from French). [PubMed: 17762825]

Montcouquiol M, Crenshaw EB 3rd, Kelley MW. Noncanonical Wnt signaling and neural polarity. Annu Rev Neurosci. 2006; 29:363–386. [PubMed: 16776590]

Montcouquiol M, Jones JM, Sans N. Detection of planar polarity proteins in mammalian cochlea. Methods Mol Biol (Clifton, NJ). 2008; 468:207–219.

Mozaffarian D, Rimm EB. Fish intake, contaminants, and human health: evaluating the risks and the benefits. Jama. 2006; 296:1885–1899. [PubMed: 17047219]

Murdoch JN, Doudney K, Paternotte C, Copp AJ, Stanier P. Severe neural tube defects in the loop-tail mouse result from mutation of Lpp1, a novel gene involved in floor plate specification. Human molecular genetics. 2001; 10:2593–2601. [PubMed: 11709546]

Myers GJ, Davidson PW. Prenatal methylmercury exposure and children: neurologic, developmental, and behavioral research. Environ Health Perspect. 1998; 106(Suppl 3):841–847. [PubMed: 9646047]

Myers GJ, Davidson PW, Shamlaye CF. A review of methylmercury and child development. Neurotoxicology. 1998; 19:313–328. [PubMed: 9553968]

National Research Council (US). Commission on Life Sciences., National Research Council (US). Scientific frontiers in developmental toxicology and risk assessment. Vol. xviii. Washington, DC: National Academy Press; 2000. Committee on Developmental Toxicology; 327 p.

O′Hara MF, Charlap JH, Craig RC, Knudsen TB. Mitochondrial transduction of ocular teratogenesis during methylmercury exposure. Teratology. 2002; 65:131–144. [PubMed: 11877777]

Olson FC, Massaro EJ. Effects of methyl mercury on murine fetal amino acid uptake, protein synthesis and palate closure. Teratology. 1977; 16:187–194. [PubMed: 929435]

Olson FC, Massaro EJ. Developmental pattern of cAMP, adenyl cyclase, and cAMP phosphodiesterase in the palate, lung, and liver of the fetal mouse: alterations resulting from exposure to methylmercury at levels inhibiting palate closure. Teratology. 1980; 22:155–166. [PubMed: 6255623]

Oshita A, Kishida S, Kobayashi H, Michiue T, Asahara T, Asashima M, Kikuchi A. Identification and characterization of a novel Dvl-binding protein that suppresses Wnt signalling pathway. Genes Cells. 2003; 8:1005–1017. [PubMed: 14750955]

Ou YC, Thompson SA, Kirchner SC, Kavanagh TJ, Faustman EM. Induction of growth arrest and DNA damage-inducible genes Gadd45 and Gadd153 in primary rodent embryonic cells following exposure to methylmercury. Toxicol Appl Pharmacol. 1997; 147:31–38. [PubMed: 9356304]

Ou YC, Thompson SA, Ponce RA, Schroeder J, Kavanagh TJ, Faustman EM. Induction of the cell cycle regulatory gene p21 (Waf1, Cip1) following methylmercury exposure in vitro and in vivo. Toxicol Appl Pharmacol. 1999; 157:203–212. [PubMed: 10373404]

Papaconstantinou AD, Brown KM, Noren BT, McAlister T, Fisher BR, Goering PL. Mercury, cadmium, and arsenite enhance heat shock protein synthesis in chick embryos prior to embryotoxicity. Birth Defects Res B Dev Reprod Toxicol. 2003; 68:456–464. [PubMed: 14745979]

Ponce RA, Kavanagh TJ, Mottet NK, Whittaker SG, Faustman EM. Effects of methyl mercury on the cell cycle of primary rat CNS cells in vitro. Toxicol Appl Pharmacol. 1994; 127:83–90. [PubMed: 8048057]

Qian D, Jones C, Rzadzinska A, Mark S, Zhang X, Steel KP, Dai X, Chen P. Wnt5a functions in planar cell polarity regulation in mice. Dev Biol. 2007; 306:121–133. [PubMed: 17433286]

Robinson JF, Yu X, Hong S, Griffith WC, Beyer R, Kim E, Faustman EM. Cadmium-induced differential toxicogenomic response in resistant and sensitive mouse strains undergoing neurulation. Toxicol Sci. 2009; 107:206–219. [PubMed: 18974090]

Rodier PM. Developing brain as a target of toxicity. Environ Health Perspect. 1995; 103(Suppl 6):73–76. [PubMed: 8549496]

Ruiz i Altaba A, Nguyen V, Palma V. The emergent design of the neural tube: prepattern, SHH morphogen and GLI code. Current Opin Genet Dev. 2003; 13:513–521.

Spyker JM, Smithberg M. Effects of methylmercury on prenatal development in mice. Teratology. 1972; 5:181–190. [PubMed: 4623447]

Stoltenburg-Didinger G, Markwort S. Prenatal methylmercury exposure results in dendritic spine dysgenesis in rats. Neurotoxicol Teratol. 1990; 12:573–576. [PubMed: 2255299]

Stone DM, Murone M, Luoh S, Ye W, Armanini MP, Gurney A, Phillips H, Brush J, Goddard A, de Sauvage FJ, Rosenthal A. Characterization of the human suppressor of fused, a negative regulator of the zinc-finger transcription factor Gli. J Cell Sci. 1999; 112:4437–4448. [PubMed: 10564661]

Stummann TC, Hareng L, Bremer S. Hazard assessment of methylmercury toxicity to neuronal induction in embryogenesis using human embryonic stem cells. Toxicology. 2009; 257:117–126. [PubMed: 19150642]

Su MQ, Okita GT. Behavioral effects on the progeny of mice treated with methylmercury. Toxicol Appl Pharmacol. 1976a; 38:195–205. [PubMed: 982468]

Su MQ, Okita GT. Embryocidal and teratogenic effects of methylmercury in mice. Toxicol Appl Pharmacol. 1976b; 38:207–216. [PubMed: 982469]

Tamm C, Duckworth J, Hermanson O, Ceccatelli S. High susceptibility of neural stem cells to methylmercury toxicity: effects on cell survival and neuronal differentiation. J Neurochem. 2006; 97:69–78. [PubMed: 16524380]

Tissir F, Goffinet AM. Expression of planar cell polarity genes during development of the mouse CNS. Eur J Neurosci. 2006; 23:597–607. [PubMed: 16487141]

Tissir F, De-Backer O, Goffinet AM, Lambert de Rouvroit C. Developmental expression profiles of Celsr (Flamingo) genes in the mouse. Mechan Dev. 2002; 112:157–160.

Torban E, Patenaude AM, Leclerc S, Rakowiecki S, Gauthier S, Andelfinger G, Epstein DJ, Gros P. Genetic interaction between members of the Vangl family causes neural tube defects in mice. Proc Natl Acad Sci USA. 2008; 105:3449–3454. [PubMed: 18296642]

Wawrzak D, Metioui M, Willems E, Hendrickx M, de Genst E, Leyns L. Wnt3a binds to several sFRPs in the nanomolar range. Biochem Biophys Res Commun. 2007; 357:1119–1123. [PubMed: 17462603]

Wlodarczyk BJ, Cabrera RM, Hill DS, Bozinov D, Zhu H, Finnell RH. Arsenic-induced gene expression changes in the neural tube of folate transport defective mouse embryos. Neurotoxicology. 2006; 27:547–557. [PubMed: 16620997]

Yu X, Griffith WC, Hanspers K, Dillman JF, Ong H 3rd, Vredevoogd MA, Faustman EM. A system-based approach to interpret dose- and time-dependent microarray data: quantitative integration of gene ontology analysis for risk assessment. Toxicol Sci. 2006; 92:560–577. [PubMed: 16601082]

Yue S, Chen Y, Cheng SY. Hedgehog signaling promotes the degradation of tumor suppressor Sufu through the ubiquitin-proteasome pathway. Oncogene. 2009; 28:492–499. [PubMed: 18997815]

Zhou L, Tissir F, Goffinet AM. The atypical cadherin Celsr3 regulates the development of the axonal blueprint. Novartis Foundation Symposium. 2007; 288:130–134. discussion 134–140, 181–276. [PubMed: 18494256]

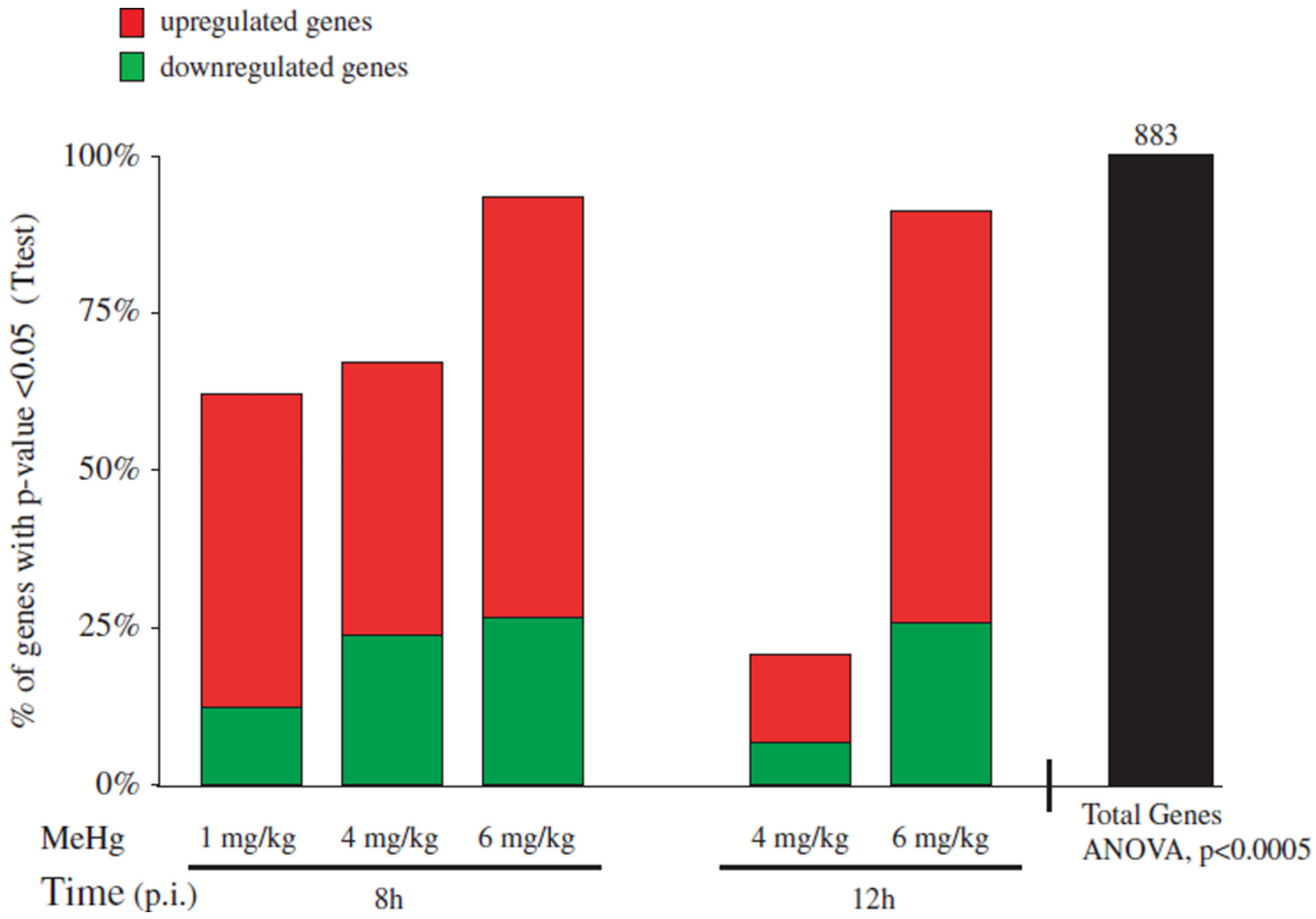

Fig. 1.

Dose- and time-dependent MeHg-induced gene expression alterations in C57 embryos. Using Model 1, we identified 883 genes to be significantly altered by MeHg (F-test, B_{MeHg}, $P<0.0005$) across time (black bar, far right). Within these 883 genes, post-hoc analyses (*t*-test) were conducted to identify the number of genes within each treatment group to be significantly altered in comparison with appropriate control (8 or 12 h post-injection). The percentage of genes with a *P* value (*t*-test) less than 0.05 are displayed in comparison with the total amount of genes identified to be significantly altered across all dose groups. The percentage of up- and downregulated genes is indicated by color (red, upregulated; green, downregulated).

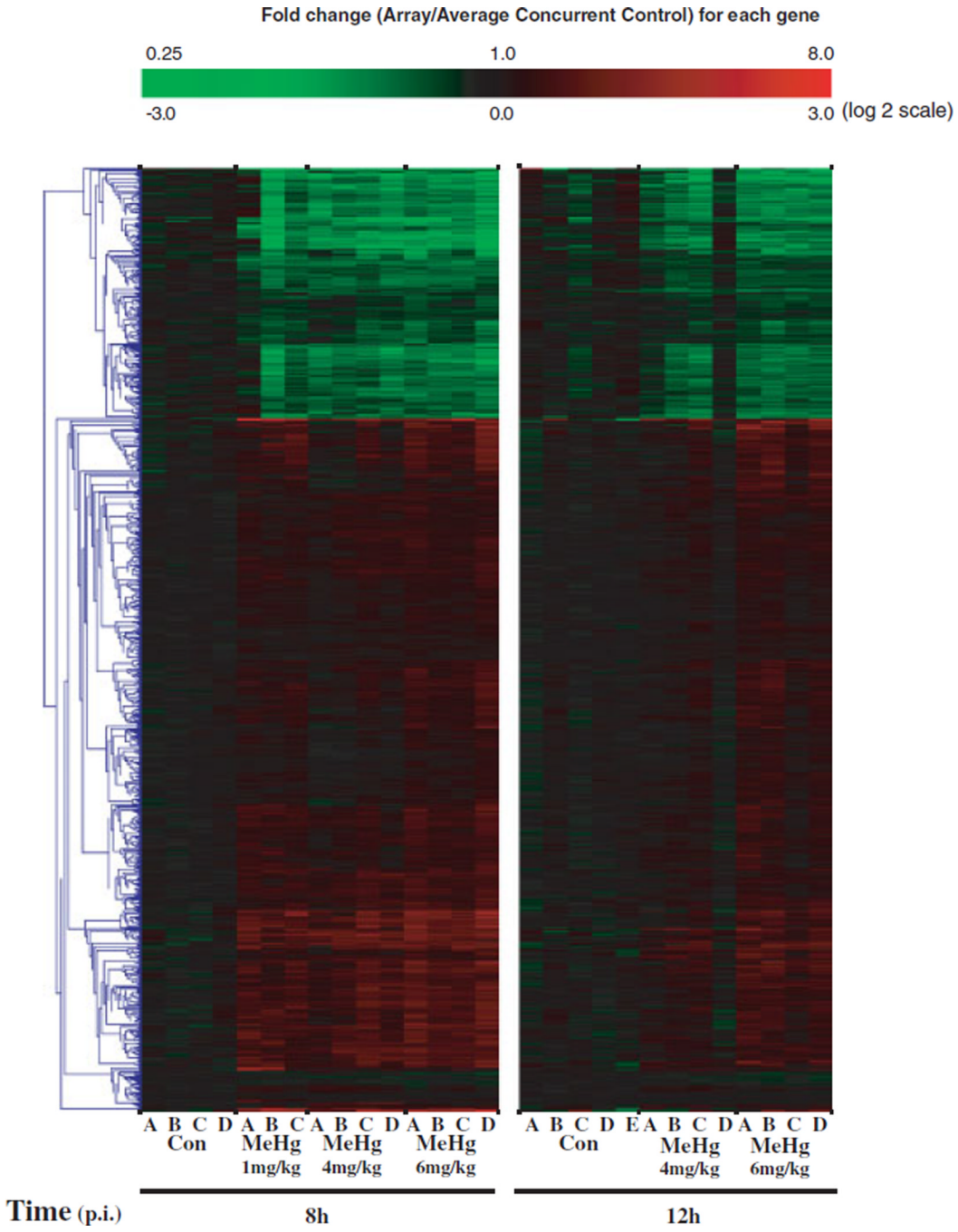

Fig. 2.

Hierarchical clustering analysis of dose- and time-dependent MeHg-induced gene expression alterations C57 embryos. Hierarchical clustering was completed using average linkage and Euclidean dissimilarity methods (TIGR MEV) on all 883 genes identified to be altered by MeHg across time (B_{MeHg}, $P<0.0005$). Log_2 ratios were determined between each array and their respective average control (8 or 12 h). The blue lines represent the gene clustering tree. Genes clustered together show similar relationships across the 28 arrays. Arrays from the Con 0h exposure group are not shown.

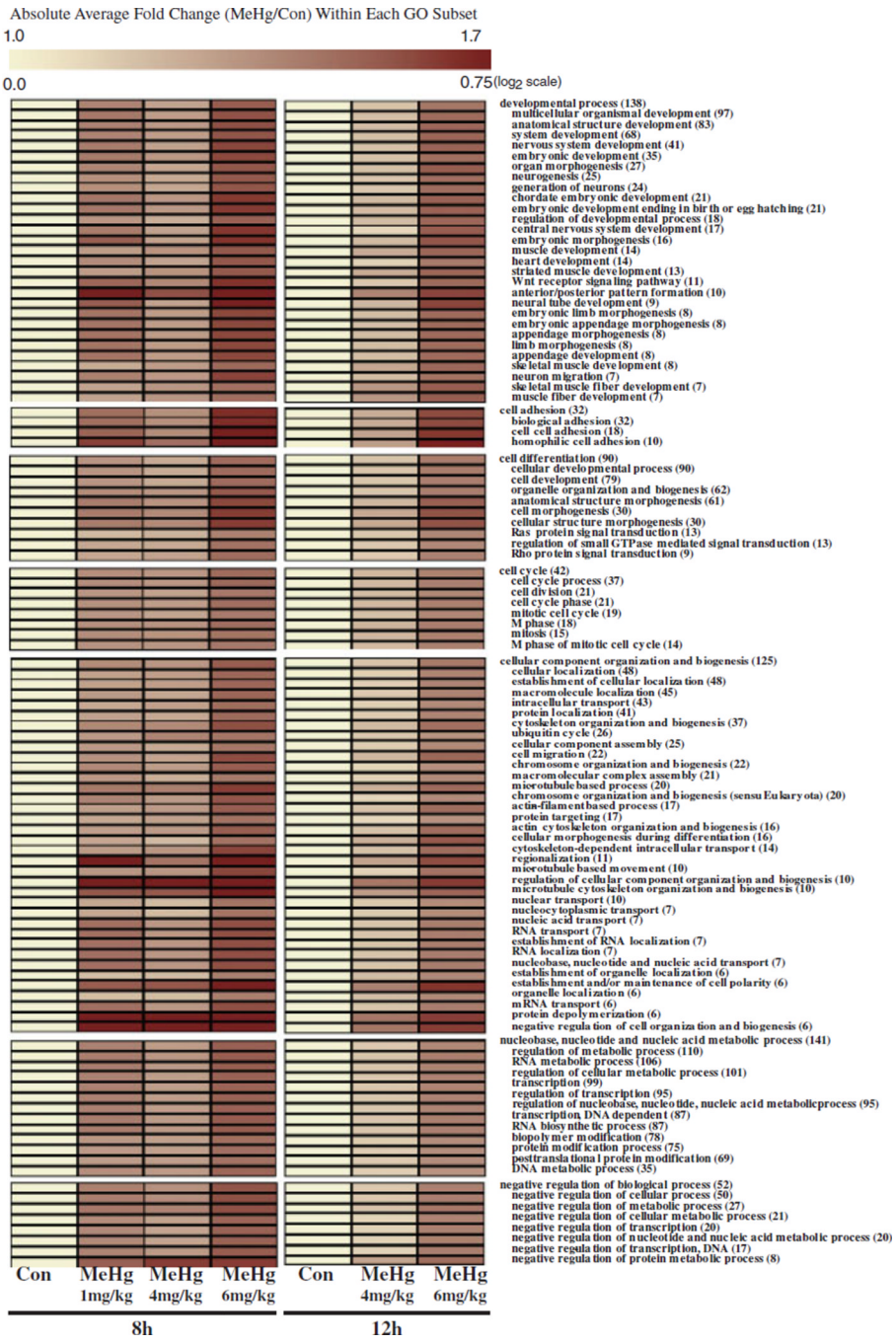

Fig. 3.

GO-quant analysis of enriched GO biological processes/pathways across dose and time. GO analysis was performed to identify enriched biological processes (GO, MAPPFinder) within genes identified to be significantly altered with MeHg across time (B_{MeHg}, $P<0.0005$). One hundred and eight categories were identified to be enriched based on the following criteria (number changed >5, Z-score >2, $P<0.001$). The absolute average ratio of gene expression response for genes within each enriched GO category was calculated using GO-Quant across dose and time and depicted by color using TIGR MEV. The total amount of genes significantly altered by MeHg within each GO category is located next to each GO term in parenthesis (X). Families of categorical terms are separated by white space.

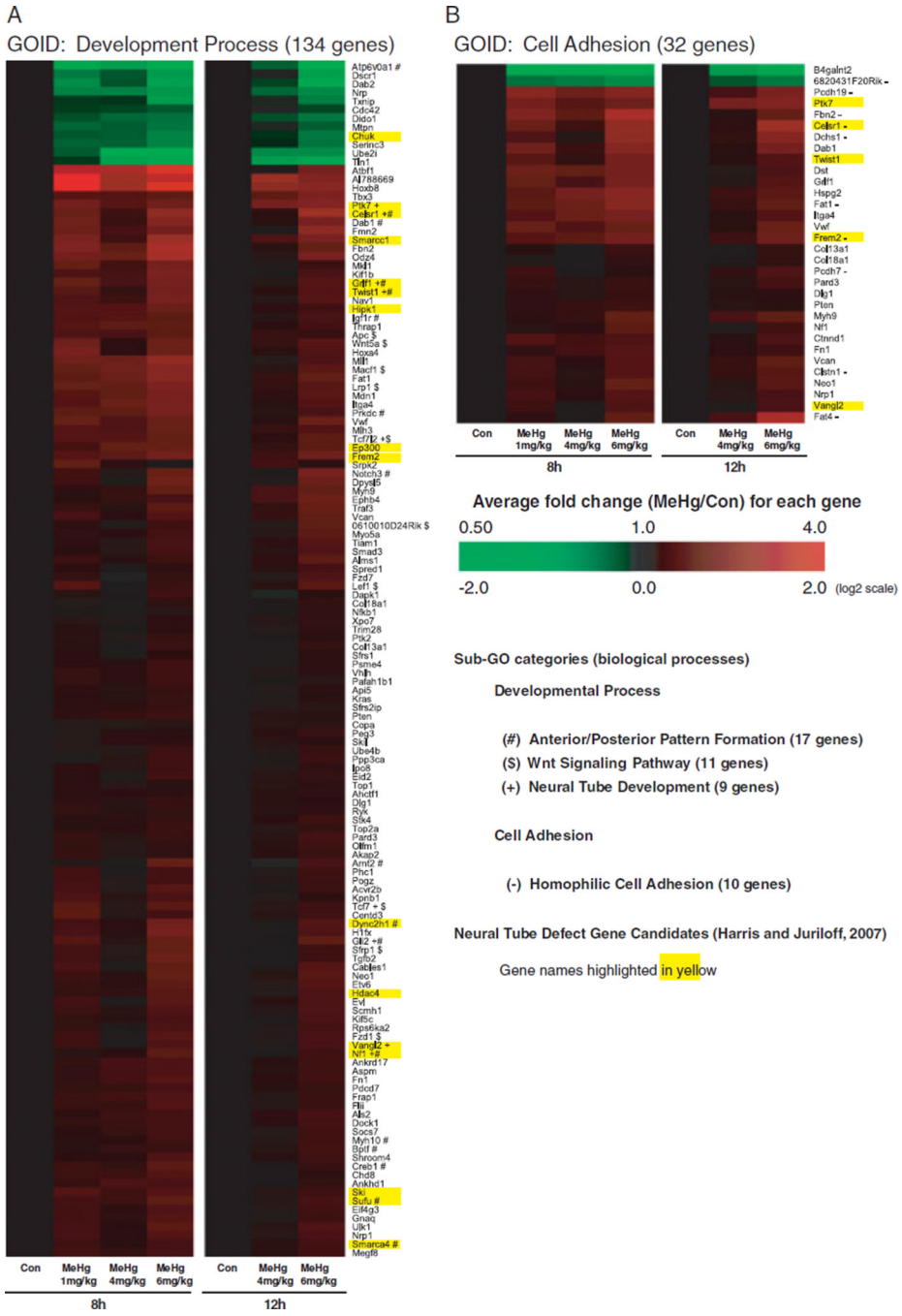

Fig. 4.

Hierarchical clustering analysis of dose- and time-dependent MeHg-induced gene expression alterations related to development (**A**) and cell adhesion (**B**). Hierarchical clustering was completed using average linkage and Euclidean dissimilarity methods (TIGR MEV) for all significant genes ($P < 0.0005$) altered by MeHg associated with the GO term developmental process (A) and cell adhesion (B). Log_2 ratios were determined between the average of each treatment group and their respective average control (8 or 12 h). Subcategories of the GO term "developmental process" related to neurulation are labeled, (+) neural tube development, ($) anterior/posterior pattern formation, ($) Wnt-signaling

pathway. Genes related to the subcategory “homophilic cell adhesion” are indicated (−) in B. Genes previously linked with neural tube defects in mouse models (Juriloff and Harris, 2008) are highlighted in yellow.

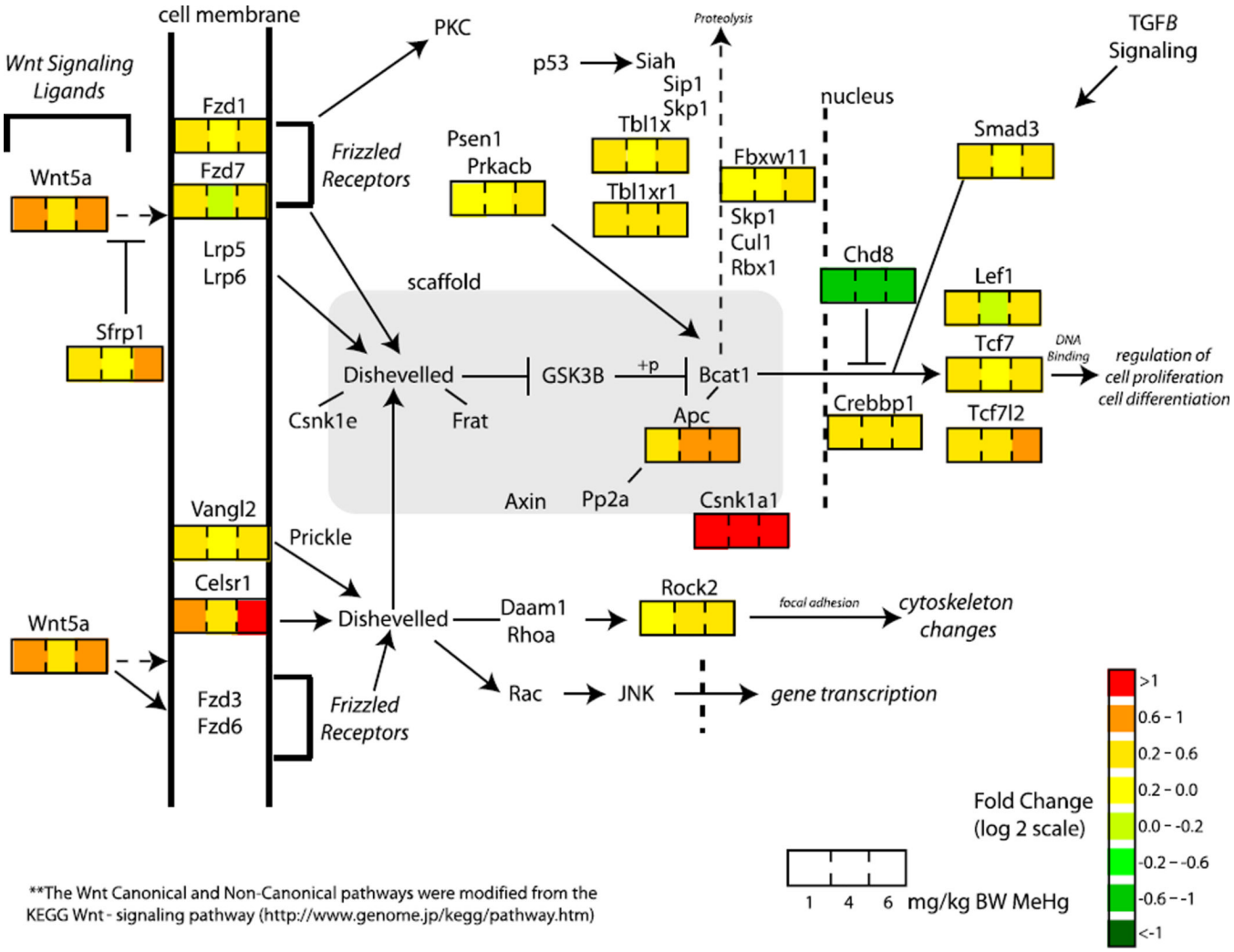

Fig. 5.

Dose-dependent MeHg-induced gene expression alterations within the Wnt-signaling pathway. The degree of impact by MeHg is displayed in genes identified to be significantly altered by MeHg (ANOVA, $P<0.0005$) and linked with the Wnt Signaling Pathway (Dennis et al., 2003). Each gene is color coded based on fold change of response (log 2 scale) for each gene with 1, 4, and 6 mg/kg BW MeHg, respectively. Only fold change values associated with 8 h exposure data are displayed. Fold change values are not present for genes identified to be not significantly altered by MeHg. Pathways were generated via the Wnt-signaling pathway (http://www.genome.jp/) with modifications, including the addition of genes, Wnt5a and Celsr1 to the Non-Canonical Wnt-signaling pathway due to recent studies suggesting an important role in activation of this pathway (Montcouquiol, 2007; Montcouquiol et al., 2006, 2008; Qian et al., 2007; Tissir and Goffinet, 2006; Zhou et al., 2007). The Wnt-signaling pathway represented the most enriched KEGG pathway within genes significantly altered by MeHg.

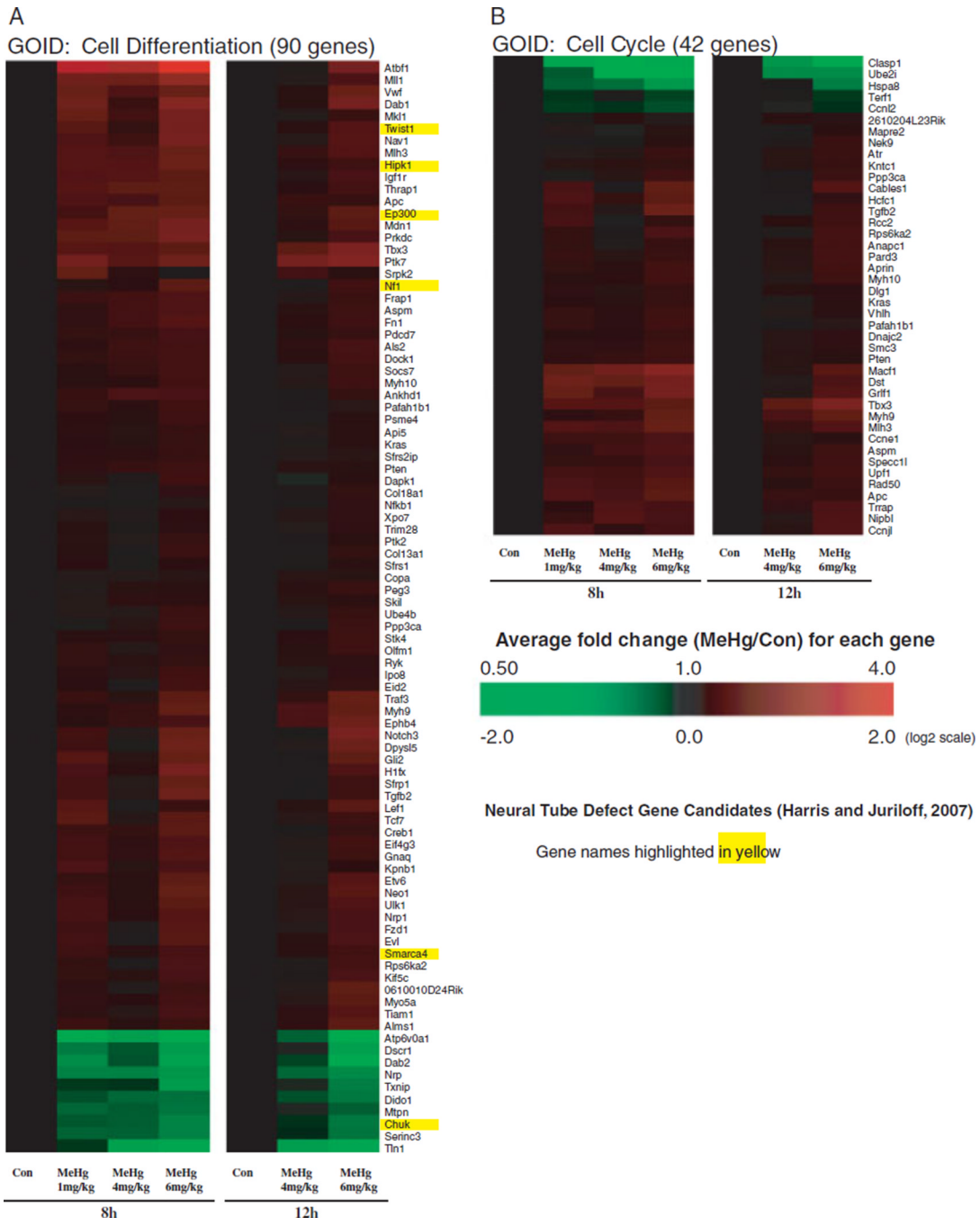

Fig. 6.

Hierarchical clustering analysis of dose- and time-dependent MeHg-induced gene expression alterations related to cell differentiation (**A**) and cell cycle (**B**). Hierarchical clustering was completed using average linkage and Euclidean dissimilarity methods (TIGR MEV) on all significant genes (B_{MeHg}, $P<0.0005$) altered by MeHg associated with the GO term cell differentiation (A) and cell cycle (B). Log_2 ratios were determined between each array and their respective average control (8 or 12h).